

First evidence of an octupole rotational band in Ge isotopes

C. G. Wang,^{1,2,*} R. Han,^{3,*} C. Xu,^{1,†} H. Hua,^{1,‡} R. A. Bark,⁴ S. Q. Zhang,¹ S. Y. Wang,⁵ T. M. Shneidman,^{6,7} S. G. Zhou,^{3,8,9,10} J. Meng,¹ S. M. Wyngaardt,¹¹ A. C. Dai,¹ F. R. Xu,¹ X. Q. Li,¹ Z. H. Li,¹ Y. L. Ye,¹ D. X. Jiang,¹ C. G. Li,¹ C. Y. Niu,¹ Z. Q. Chen,¹ H. Y. Wu,¹ D. W. Luo,¹ S. Wang,⁵ D. P. Sun,⁵ C. Liu,⁵ Z. Q. Li,⁵ N. B. Zhang,⁵ R. J. Guo,⁵ P. Jones,⁴ E. A. Lawrie,^{4,12} J. J. Lawrie,⁴ J. F. Sharpey-Schafer,¹² M. Wiedeking,^{4,13} S. N. T. Majola,^{4,14} T. D. Bucher,^{4,11} T. Dinoko,⁴ B. Maqabuka,^{4,12} L. Makhathini,^{4,11} L. Mdletshe,^{4,15} O. Shirinda,⁴ and K. Sowazi⁴

¹School of Physics and State Key Laboratory of Nuclear Physics and Technology, Peking University, Beijing 100871, China

²Institute of Advanced Science Facilities, Shenzhen, Guangdong 518107, China

³CAS Key Laboratory of Theoretical Physics, Institute of Theoretical Physics, Chinese Academy of Sciences, Beijing 100190, China

⁴iThemba LABS, National Research Foundation, P.O. Box 722, 7129 Somerset West, South Africa

⁵Shandong Provincial Key Laboratory of Optical Astronomy and Solar-Terrestrial Environment, Institute of Space Sciences, Shandong University, Weihai 264209, China

⁶Bogoliubov Laboratory of Theoretical Physics, Joint Institute for Nuclear Research, Dubna 141980, Russia

⁷Kazan Federal University, Kazan 420008, Russia

⁸School of Physical Sciences, University of Chinese Academy of Sciences, Beijing 100049, China

⁹Center of Theoretical Nuclear Physics, National Laboratory of Heavy Ion Accelerator, Lanzhou 730000, China

¹⁰Synergetic Innovation Center for Quantum Effects and Application, Hunan Normal University, Changsha 410081, China

¹¹Department of Physics, University of Stellenbosch, Matieland 7602, South Africa

¹²Department of Physics, University of the Western Cape, P/B X17 Bellville 7535, South Africa

¹³School of Physics, University of the Witwatersrand, Johannesburg 2050, South Africa

¹⁴Department of Physics, University of Johannesburg, P.O. Box 524, Auckland Park 2006, South Africa

¹⁵Department of Physics, University of Zululand, Private Bag X1001, KwaDlangezwa 3886, South Africa

 (Received 5 October 2020; revised 2 January 2021; accepted 24 June 2022; published 20 July 2022)

The spectroscopy of ^{71}Ge has been investigated via the fusion-evaporation reaction $^{74}\text{Ge}(\alpha, \alpha 3n)^{71}\text{Ge}$. Collective structures including a rotational band built on the $15/2^-$ octupole state in ^{71}Ge have been established. The observation of strong $E1$ transitions and the well-behaved rotational sequence built on the $15/2^-$ octupole state provide the first experimental evidence of an octupole rotational band in Ge isotopes, suggesting an enhanced octupole correlation around $N = 40$ in the $A \approx 70$ region. A newly developed semimicroscopic cluster model provides a good description of the octupole characteristics of ^{71}Ge .

DOI: [10.1103/PhysRevC.106.L011303](https://doi.org/10.1103/PhysRevC.106.L011303)

As one of the fundamental properties of atomic nuclei, symmetries of nuclear shapes have long been of great interest in nuclear structure physics. Throughout the nuclear chart, most nuclei are known to have reflection-symmetric shapes. With the breaking of reflection symmetry in the intrinsic frame, some nuclei appear to have an octupole deformation, i.e., pearlike shapes [1,2]. The occurrence of octupole deformations can be ascribed to the strong coupling between the orbitals in the intruder subshell (l, j) and the orbitals in the normal-parity subshell ($l-3, j-3$). Nazarewicz *et al.* have proposed that the nuclei with maximal octupole coupling (i.e., the best candidates for static octupole deformation) occur when particle numbers are around 34, 56, 88, and 134, which were called the “octupole driving particle numbers” (ODPNs) [3]. To date, clear experimental evidence of octupole defor-

mation has been found in the $A \approx 145$ and 225 regions [4–6], showing that the ODPNs 56, 88, and 134 are fully justified. The explorations of strong octupole effects in other mass regions are still in progress [2,7].

Recently, particular attention has been paid to nuclei in the $A \approx 70$ mass region. Octupole correlations between multiple chiral doublet bands have been observed in ^{78}Br [8], which indicates that the simultaneous breaking of space reflection symmetry and chiral symmetry is possible in one single nucleus. In this region, octupole correlations are associated with the $g_{9/2}$ and $p_{3/2}$ subshells. The Strutinsky calculations by Nazarewicz *et al.* have suggested that the light Ge and Se isotopes would be stable but rather soft with respect to octupole deformation [3,9]. Systematic investigations on the behavior of the 3^- octupole states by Cottle [10] revealed that the best candidates for the maximal octupole collectivity in the light Ge and Se isotopes are $N = 40$ isotones ^{72}Ge , ^{74}Se , and neighboring nuclei. Mean-field calculations [7] and Skyrme Hartree-Fock-Bogoliubov (HFB) calculations [11] have also shown that octupole deformation may occur around $N = 40$.

*These authors equally contributed to this work.

†chuan@pku.edu.cn

‡hhua@pku.edu.cn

In general, the experimental fingerprints of strong octupole correlations [2,9] are the observation of enhanced $E1$ and/or $E3$ transitions linking the excited bands to alternating opposite-parity yrast bands, as well as the presence of octupole bands with normally ordered levels built upon 3^- octupole states in even-even nuclei or octupole states in odd- A nuclei (i.e., $15/2^-$ from the coupling of the intruded $g_{9/2}$ particle to the 3^- octupole state in the $A \approx 70$ mass region). For the Se isotopes, such an octupole rotational band built on a 3^- octupole state has already been observed in ^{74}Se [12,13]. In contrast, although a negative-parity band above the 3^- octupole state has been established in ^{72}Ge , detailed analyses suggested that this sequence may have a multiquasiparticle structure rather than be a pure octupole rotational band [14,15]. This situation also happens in the lighter even- A $^{66-70}\text{Ge}$ isotopes [16–18]. For the odd- A Ge isotopes, the experimental information about the negative-parity bands is somewhat scarce and very often only several irregularly spaced negative-parity levels above the $15/2^-$ octupole states are known [19]. Therefore, no firm evidence of an octupole rotational band in Ge isotopes has been found to date. Further exploring the octupole collectivity in the $A \approx 70$ region, especially around $N = 40$, will be crucial to answer the long-standing question to what extent the octupole collectivities would manifest themselves in the $A \approx 70$ region.

In this Letter, we report an experimental investigation of the collective structure of odd- A ^{71}Ge via the $^{74}\text{Ge}(\alpha, \alpha 3n)^{71}\text{Ge}$ fusion-evaporation reaction. In the previous spectroscopy studies of ^{71}Ge , only some individual states were observed [20]. In the present work, a rotational band built on the $15/2^-$ octupole state in ^{71}Ge is established. The observation of the strong $E1$ transitions and the well-behaved rotational sequence above the $15/2^-$ octupole state provide the first experimental evidence of an octupole rotational band in the Ge isotopes. The octupole properties of ^{71}Ge are investigated in terms of a newly developed semimicroscopic cluster model.

The present experiment was performed at the Separated Sector Cyclotron of iThemba LABS in South Africa. The high-spin states of ^{71}Ge were populated via the $^{74}\text{Ge}(\alpha, \alpha 3n)^{71}\text{Ge}$ fusion-evaporation reaction at beam energies of 58.6 and 62.6 MeV. The target consisted of a 2.85-mg/cm^2 ^{74}Ge metallic foil with a 10.80-mg/cm^2 carbon backing. In-beam γ rays were measured with the AFRODITE array [21], which consisted of eight Compton-suppressed clover detectors and two low-energy photon spectrometers at the time of the experiment. The clover detectors were arranged in two rings at 90° (four clovers) and 135° (four clovers) with respect to the beam direction.

Approximately 1.9×10^9 γ - γ coincident events were collected, from which a symmetric matrix was built. The level scheme analysis was performed using the RADWARE package [22]. To determine the multipolarities of the γ -ray transitions, two asymmetric angular distributions from oriented states (ADO) [23] matrices were constructed by using the γ rays detected at all angles (the y axis) against those detected at 90° and 135° (the x axis), respectively. The multipolarities of the emitted γ rays were analyzed by means of the ADO ratio, which was defined as $I_\gamma(\text{at } 135^\circ)/I_\gamma(\text{at } 90^\circ)$. The

TABLE I. The measured ADO ratios (R_{ADO}) and the linear polarizations for the linking transitions between band 2 and bands 1,3,4.

$E_\gamma(\text{keV})$	R_{ADO}	Linear polarization	$I_i^\pi \rightarrow I_f^\pi$
314.1	0.78(12)	0.21(8)	$19/2^- \rightarrow 17/2^+$
521.1	1.65(18)		$19/2^- \rightarrow 15/2^-$
877.8	0.68(17)		$15/2^- \rightarrow 13/2^+$
887.6	1.43(9)		$15/2^- \rightarrow 11/2^-$
923.4	1.28(9)	0.43(9)	$17/2^- \rightarrow 13/2^-$
1113.1	0.57(10)		$19/2^- \rightarrow 17/2^+$
1664.7	0.79(7)	0.34(16)	$15/2^- \rightarrow 13/2^+$

typical ADO ratios for stretched quadrupole and stretched pure dipole transitions are found to be ≈ 1.2 and ≈ 0.8 , respectively. Furthermore, to distinguish the electric and magnetic character of the γ rays, the linear polarization measurements [24] were performed using the four clover detectors positioned at 90° relative to the beam direction as Compton polarimeters.

The partial level scheme of ^{71}Ge deduced from the present work is shown in Fig. 1. It was constructed from the γ - γ coincidence relationships, intensity balances, ADO ratios, and linear polarizations. The typical γ -ray spectra which support the proposed level scheme are shown in Fig. 2. For the light odd- A Ge isotopes, the $p_{1/2}$, $p_{3/2}$, $f_{5/2}$, and $g_{9/2}$ neutron orbitals are near the Fermi surface. It has been known that the negative-parity $1/2^-$ ground state, $5/2^-$ level at 174.9 keV, and $3/2^-$ level at 499.9 keV (bandhead of band 1) in ^{71}Ge have major $p_{1/2}$, $f_{5/2}$, and $p_{3/2}$ configurations, respectively, while the positive-parity $9/2^+$ level at 198.4 keV and $7/2^+$ level at 589.7 keV (bandheads of bands 3 and 4, respectively) have the major $g_{9/2}$ components [25–27]. The low-lying levels below 2.4 MeV shown in Fig. 1 have been identified in many previous experiments, and spin-parities have been assigned to most of these levels except the 1949.3-keV level of band 1 [20]. The present analyses confirm these low-lying levels and support the previous spin-parity assignments. As shown in Figs. 2(a)–2(d), with the gates on the known γ -ray transitions in ^{71}Ge , many new coincident γ -ray transitions in bands 1, 2, 3, and 4 are observed. The present ADO analyses suggest that the new 941.0-, 976.2-keV transitions in band 1 and the new 574.4-, 826.2-, 1061.3-, 1175.6-, 1254.4-, 1386.8-keV transitions in band 2, as well as the new 1285.6-, 1294.1-, 1315.2-, 1416.3-, 1630.3-keV transitions in band 3 and the new 1138.1-, 1222.0-keV transitions in band 4, all have quadrupole transition characters. The γ -ray decays of 867.0, 1037.9 keV in band 1 and 1314.9 keV in band 4 for which the ADO ratios could not be extracted are also assumed to be stretched $E2$ transitions.

Here, of particular interest is the new band 2. As presented in Table I, the measured ADO value 0.79(7) and the linear polarization 0.34(16) suggest an $E1$ nature for the strong 1664.7-keV transition. Furthermore, according to the ADO value, the 887.6-keV transition decaying to the $11/2^-$ level in band 1 has a quadrupole character, while the 877.8-keV transition decaying to the $13/2^+$ level in band 4 has a dipole character. Based on these experimental results, the spin-parity

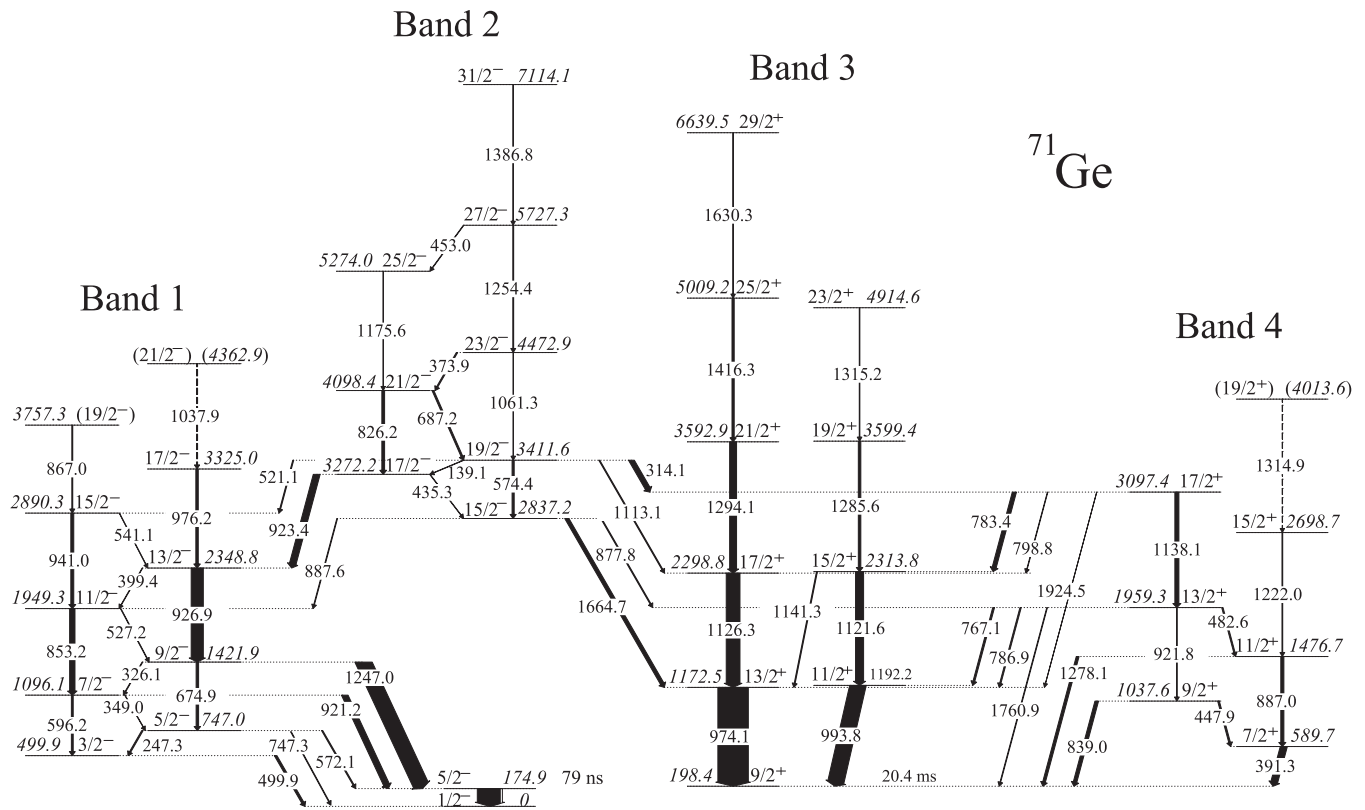


FIG. 1. Partial level scheme of ^{71}Ge . Energies are given in keV and widths of the arrows are proportional to their relative intensities.

$15/2^-$ is firmly assigned to the level at 2837.2 keV (bandhead of band 2).

The observed strong $E1$ transitions between the negative-parity band 2 and the positive-parity $g_{9/2}$ bands (3 and 4), as well as the rotational pattern built on the $15/2^-$ state, imply that the $15/2^-$ state has an octupole nature (i.e., the coupling of the $g_{9/2}$ particle to the 3^- octupole state) and that band 2 is an octupole rotational band. Figure 3(a) shows the excitation energies of the $15/2^-$ states (relative to the yrast $9/2^+$ states) in odd- A Ge isotopes [28,29], as well as the excitation energies of the 3^- states in even- A Ge isotopes [15–18,30]. It can be seen that the excitation energy of the candidate $15/2^-$ octupole state in ^{71}Ge follows the trend of smoothly decreasing energy with increasing neutron number and has the lowest observed energy in the odd- A Ge isotopes, suggesting an enhanced degree of octupole driving collectivity towards the new optimal octupole driving particle number $N = 40$ [10].

To investigate the octupole collectivity above the $15/2^-$ state, the experimental $B(E1, 314.1 \text{ keV})/B(E2, 574.4 \text{ keV})$ branching ratio of the $19/2^-$ state in ^{71}Ge is extracted and compared with those in the neighboring odd- A Ge isotopes [28,29] in Fig. 3(b), as well as that in the octupole-deformed nucleus ^{220}Ra [31]. As shown in Fig. 3(b), the ^{71}Ge nucleus has a strong $B(E1)/B(E2)$ branching ratio value of $2.76(58) \times 10^{-6} \text{ fm}^{-2}$, which is significantly larger than those of neighboring odd- A Ge isotopes and is on the same level with ^{220}Ra , indicating that ^{71}Ge can well maintain its octupole collectivity above the $15/2^-$ octupole state.

It has been suggested that, for a nucleus with stable octupole shape, pronounced alignment may be absent at frequencies where it is observed in reflection-symmetric nuclei and a delayed band crossing is expected instead [32,33]. The alignments as a function of rotational frequency for band 2 in ^{71}Ge , together with that for the negative-parity band built on the 3^- in ^{72}Ge [15], are plotted in Fig. 4. The negative-parity band in ^{72}Ge displays two obvious upbends at ≈ 0.25 MeV and ≈ 0.50 MeV, which were interpreted as transitions from octupole to two-quasiparticle structure and from two-quasiparticle to four-quasiparticle structure [15], respectively. In contrast, band 2 in ^{71}Ge shows a relatively flat behavior up to at least ≈ 0.60 MeV, which is consistent with the picture expected for the octupole rotational band [1,2]. Note that the lack of alignment in band 2 cannot be simply explained by the blocking effect of the odd neutron in ^{71}Ge , as an alignment of a $g_{9/2}$ proton pair was expected to happen at 0.5 MeV as in neighboring isotones ^{73}Se [34] and ^{75}Kr [35]. Cottle and Bignall have made a systematic investigation of the influence of nuclear rotation on the candidates of octupole bands in the even-even Zn, Ge, Se, Kr, Sr, and Zr isotopes in this region [36]. They found that only in four even-even nuclei, ^{74}Se , $^{76,78}\text{Kr}$, and ^{82}Sr , do the octupole bands persist with octupole collectivity to high angular momenta above $7\hbar$. The behavior of band 2 in ^{71}Ge up to the largest observed spin indicates that the octupole nature in ^{71}Ge can also be retained to high angular momenta as in ^{74}Se , $^{76,78}\text{Kr}$, and ^{82}Sr , which provides a first candidate of an octupole rotational band in the odd- A nuclei in this region.

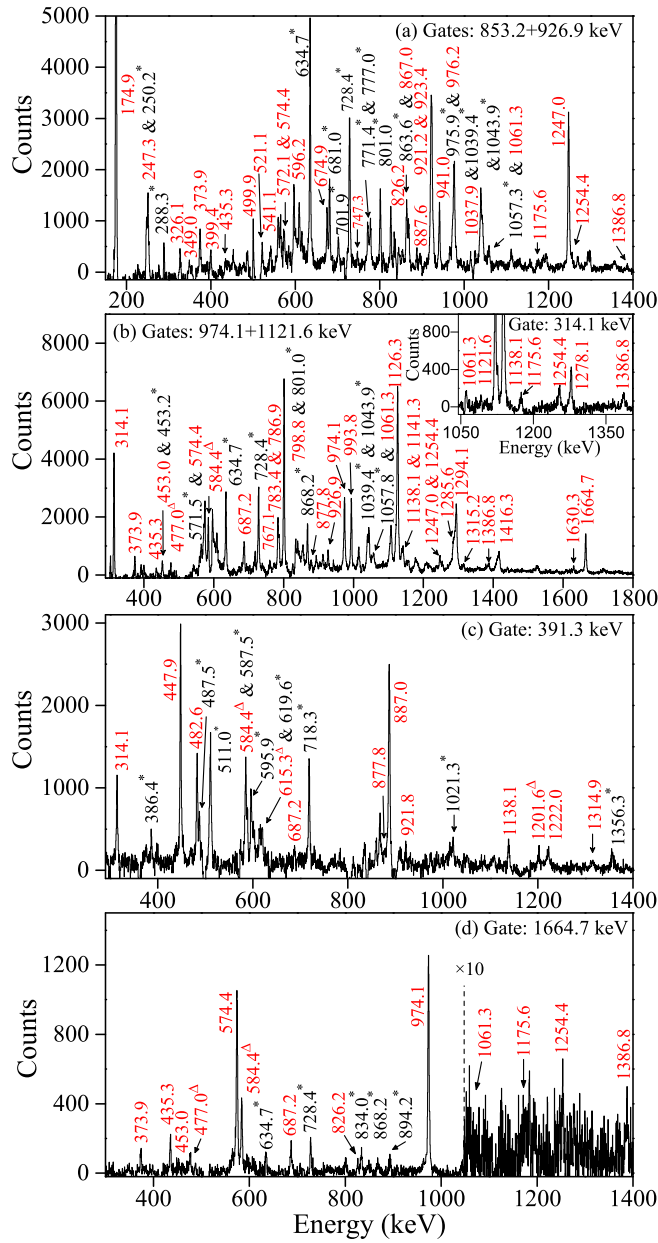


FIG. 2. Coincident spectra for ^{71}Ge , gated on the (a) 853.2 + 926.9 keV transitions, (b) 974.1 + 1121.6 keV transitions, (c) 391.3 keV transition, and (d) 1664.7 keV transition. Transitions of ^{71}Ge are marked in red. The peaks marked with asterisks are known contaminants, and the peaks marked with triangles are not included in the partial level scheme of Fig. 1. The inset in (b): Coincident γ -ray spectrum gated on the 314.1 keV transition.

To further investigate the octupole properties in ^{71}Ge , theoretical calculations have been performed with a newly developed semimicroscopic cluster model for odd- A systems [37]. The Hamiltonian consists of the rotational and vibrational energies of the even-even core, the quasiparticle energies, and the coupling between the core and the valence particle. The collective motion of the even-even core is described in the framework of the dinuclear system (DNS) [38–43] on the assumption that cluster-type shapes are

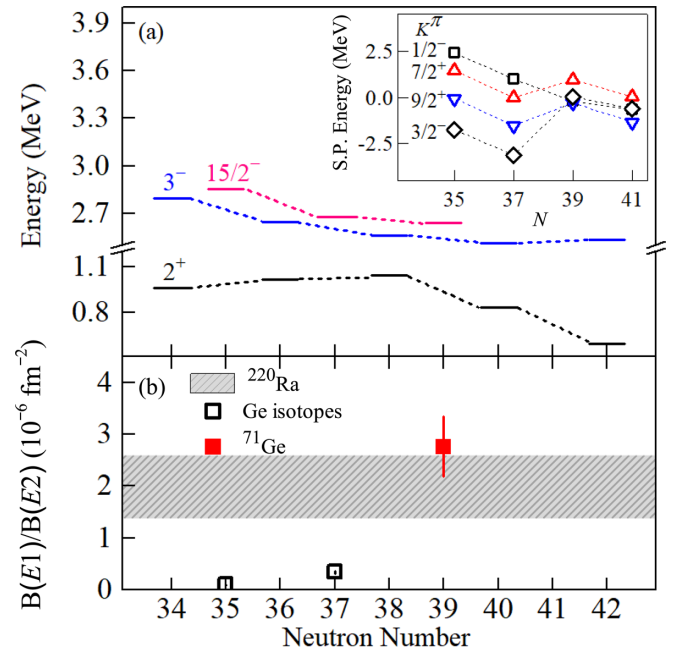


FIG. 3. (a) Excitation energies of the $15/2^-$ states (relative to the yrast $9/2^+$ states) in odd- A Ge isotopes [28,29], and the 3^- and 2^+ states in even- A Ge isotopes [15–18,30]. (b) The experimental $B(E1)/B(E2)$ branching ratios of $19/2^-$ state in ^{71}Ge in comparison with experimental values in the neighboring odd- A Ge isotopes deduced from [28,29], and the octupole-deformed nucleus ^{220}Ra deduced from [31]. The average $B(E1)/B(E2)$ branching ratio with experimental uncertainty for the octupole band in ^{220}Ra is displayed as the shaded region. Inset in (a): The neutron single-particle levels originating from the $g_{9/2}$ and $p_{3/2}$ orbitals in odd- A Ge isotopes.

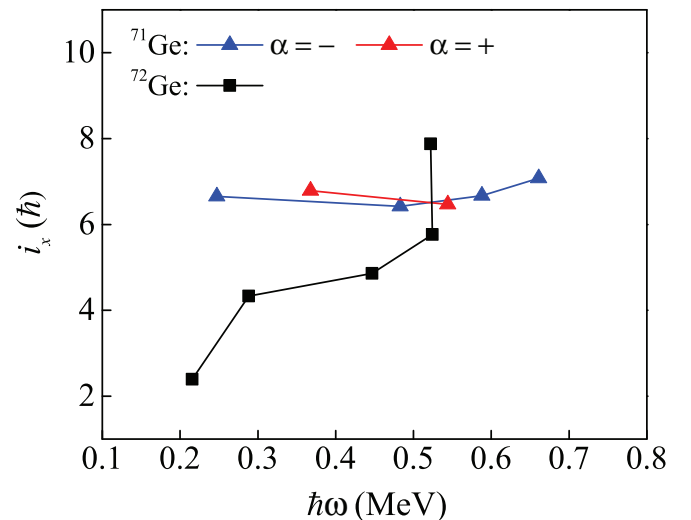


FIG. 4. Aligned spins as a function of the rotational frequency for bands 2 in ^{71}Ge and the negative-parity band in ^{72}Ge [14,15]. Harris parameters of $J_0 = 3.5\hbar^2/\text{MeV}$ and $J_1 = 17.0\hbar^4/\text{MeV}^3$ have been assumed.

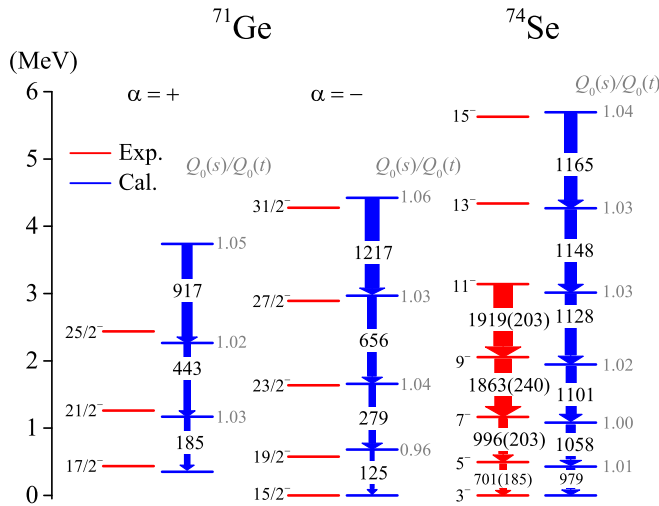


FIG. 5. The calculated excitation energies (in MeV) and intra-band $B(E2)$ values (in $e^2\text{fm}^4$) are compared with the experimental data of the octupole bands in ^{71}Ge and ^{74}Se . The ratios of the intrinsic quadrupole moments $Q_0(s)$ (from spectroscopic properties) and $Q_0(t)$ (from $E2$ transitions) are shown on the right side of the calculated levels. The experimental data of ^{74}Se are taken from Ref. [13].

produced by the motion of the system in the mass-asymmetry degree of freedom. The mass-asymmetry is defined as $(A_1 - A_2)/(A_1 + A_2)$ [39], where A_1 and A_2 represent the masses of two clusters. The quasiparticle energies are obtained from the two-center shell model (TCSM) [44] at the deformations corresponding to the minimum of the potential energy surface. In view of quadrupole and octupole degrees of freedom in this region, to provide an appropriate description of the coupling between the core and the valence particle for odd- A nuclei, here, the coupling term is expanded in multipoles (quadrupole and octupole) as in Ref. [45].

For ^{71}Ge , TCSM predicts the ground state minimum with the quadrupole deformation $\beta_2 = -0.21$, which agrees well with the previous predictions $\beta_2 = -0.20$ by the finite-range droplet model [46]. The present calculations indicate the octupole band in ^{71}Ge is originated from the $K = 7/2^+$ quasiparticle state coupling to the $K = 0^-$ collective octupole core (with β_{30} octupole phonon excitation). Figure 5 shows the calculated results of the octupole band in ^{71}Ge along with those in ^{74}Se . The calculated spectra agree well with the experiment for both nuclei. The theoretical $B(E2)$ values increase smoothly with spin and are comparable with the experimental data in ^{74}Se [13]. The present calculations also suggest the concerned bands have good rotor characters. As is well known, the intrinsic quadrupole moment [written as $Q_0(s)$] can be deduced from the spectroscopic quadrupole moment [47]. Moreover, for the rotational states, the intrinsic quadrupole moment [written as $Q_0(t)$] can be also deduced from the $B(E2)$ value of the $E2$ transition [47]. In the case of a good deformed rotor, these two definitions of the intrinsic quadrupole moments should be equal to each other [48,49]. As shown in Fig. 5, the calculated ratios of the intrinsic

quadrupole moments $Q_0(s)$ and $Q_0(t)$ are close to unity for both bands in ^{71}Ge and ^{74}Se , revealing their good rotor characters.

The calculated $B(E1)$ value from the $19/2^-$ level of band 2 to $17/2^+$ level of band 4 is $1.0 \times 10^{-4} e^2\text{fm}^2$, which is larger than the available experimental $B(E1)$ value ($5^- \rightarrow 4^+$) of $1.6(5) \times 10^{-6} e^2\text{fm}^2$ for the octupole band in ^{74}Se [50], and lies in between the available experimental $B(E1)$ values of octupole bands in Ra isotopes around $A \approx 220$, for example it is smaller than the $3.0(11) \times 10^{-3} e^2\text{fm}^2$ value for $5^- \rightarrow 4^+$ in ^{222}Ra [51] and larger than the $9.5(71) \times 10^{-5} e^2\text{fm}^2$ value for $5^- \rightarrow 4^+$ in ^{224}Ra [4]. In addition, both the experimental observation and calculations show that the $E1$ decay probability from band 2 to band 4 is stronger than that to band 3, which may indicate that the positive-parity partner of the octupole band in ^{71}Ge is band 4.

It is well known that the octupole deformation works generally in conjunction with the dominant quadrupole deformation, which usually make pairs of orbitals with $\Delta j = \Delta l = 3$ orbitals closer in energy, allowing an enhanced octupole coupling. Recent theoretical studies for lanthanide and actinide nuclei indicate that the inclusion of the quadrupole-octupole coupling provides a good description of key octupole spectroscopic properties in these regions [52–56]. As shown in Fig. 3(a), when the neutron number increased from 38 to 40, the first 2^+ state in even- A Ge isotopes decreases rapidly, reflecting the increase of quadrupole collectivity. Here, the neutron single-particle levels with different K around the Fermi surface for odd- A Ge isotopes have been calculated by TCSM. The levels originating from the neutron $g_{9/2}$ and $p_{3/2}$ orbitals, which play a major role in octupole correlations, are plotted in the inset of Fig. 3(a). It can be seen that the spacing between these single-particle levels decreases with increase in neutron number and a high level density occurs around ^{71}Ge , which leads to the strong octupole correlation in this nucleus. So far, theoretical studies of quadrupole-octupole coupling in the $A \approx 70$ mass region have not been performed in much detail and are much anticipated in the future.

In summary, high-spin states of ^{71}Ge have been produced via the fusion-evaporation reaction $^{74}\text{Ge}(\alpha, \alpha 3n)^{71}\text{Ge}$. The collective structure of ^{71}Ge has been established and an octupole rotational band is identified for the first time based on its rotational pattern, large experimental $B(E1)/B(E2)$ branching ratios, and the lack of alignment. A newly developed semimicroscopic cluster model gives a good description of the octupole characteristics of ^{71}Ge . The octupole collective structure observed in ^{71}Ge suggests an enhanced octupole correlation around $N = 40$ in the $A \approx 70$ region, which is helpful for a comprehensive understanding of the spontaneous breaking of the fundamental spatial reflection symmetry in nuclear chart. To have a deeper insight into the distinct role of the odd nucleon in forming octupole collective structure in the light mass region, more experimental and theoretical studies are highly desired.

This work is supported by the National Key R&D Program of China under Grant No. 2018YFA0404403,

the National Science Foundation of China under Grants No. 12035001, No. 12075006, No. 11675003, No. 11875075, No. 11235001, No. 11835001, No. 11320101004, No. 11525524, No. 12070131001, and No. 11961141004, the CAS Strategic Priority Research Program (XDB34010000), RFBR (Moscow) under Grant No. 17-52-12015, and the

National Research Foundation of South Africa Grants No. 90741 and No. 92791. The computation of this work was supported by the HPC Cluster of KLTP/ITP-CAS and the Supercomputing Center, CNIC of CAS. The authors wish to thank Dr. Q. W. Fan for making the target and the staff of iThemba LABS for their support.

-
- [1] I. Ahamad and P. A. Butler, *Annu. Rev. Nucl. Part. Sci.* **43**, 71 (1993), and references therein.
- [2] P. A. Butler and W. Nazarewicz, *Rev. Mod. Phys.* **68**, 349 (1996), and references therein.
- [3] W. Nazarewicz, P. Olanders, I. Ragnarsson, J. Dudek, G. A. Leander, P. Möller, and E. Ruchowska, *Nucl. Phys. A* **429**, 269 (1984).
- [4] L. P. Gaffney *et al.*, *Nature (London)* **497**, 199 (2013).
- [5] B. Bucher *et al.*, *Phys. Rev. Lett.* **116**, 112503 (2016).
- [6] B. Bucher *et al.*, *Phys. Rev. Lett.* **118**, 152504 (2017).
- [7] L. M. Robledo and G. F. Bertsch, *Phys. Rev. C* **84**, 054302 (2011).
- [8] C. Liu *et al.*, *Phys. Rev. Lett.* **116**, 112501 (2016).
- [9] W. Nazarewicz, *Nucl. Phys. A* **520**, c333 (1990).
- [10] P. D. Cottle, *Phys. Rev. C* **42**, 1264 (1990).
- [11] Y. C. Cao, S. E. Agbemava, A. V. Afanasjev, W. Nazarewicz, and E. Olsen, *Phys. Rev. C* **102**, 024311 (2020).
- [12] R. B. Piercey, A. V. Ramayya, R. M. Ronningen, J. H. Hamilton, R. L. Robinson, and H. J. Kim, *Phys. Rev. Lett.* **37**, 496 (1976).
- [13] P. D. Cottle, J. W. Holcomb, T. D. Johnson, K. A. Stuckey, S. L. Tabor, P. C. Womble, S. G. Buccino, and F. E. Durham, *Phys. Rev. C* **42**, 1254 (1990).
- [14] D. G. Roux, K. R. Henninger, R. A. Bark, S. Bvumbi, E. A. Gueorguieva-Lawrie, S. M. Mullins, S. H. T. Murray, L. P. Masiteng, and O. Shirinda, in *Proceedings of the 32nd International Workshop on Nuclear Theory (IWNT-32)*, Rila Mountains, 2013, edited by A. Georgieva and N. Minkov (Heron, Sofia, Bulgaria), p. 181.
- [15] D. G. Roux *et al.*, *Eur. Phys. J. A* **48**, 99 (2012).
- [16] E. A. Stefanova *et al.*, *Phys. Rev. C* **67**, 054319 (2003).
- [17] D. Ward *et al.*, *Phys. Rev. C* **63**, 014301 (2000).
- [18] R. A. Haring-Kaye *et al.*, *Phys. Rev. C* **97**, 024308 (2018).
- [19] Evaluated Nuclear Structure Data File (ENSDF), <http://www.nndc.bnl.gov/ensdf>.
- [20] K. Abusaleem and B. Singh, *Nucl. Data Sheets* **112**, 133 (2011), and references therein.
- [21] J. F. Sharpey-Schafer, *Nucl. Phys. News* **14**(1), 5 (2004).
- [22] D. C. Radford, *Nucl. Instrum. Methods Phys. Res., Sect. A* **361**, 297 (1995).
- [23] M. Piiparinen *et al.*, *Nucl. Phys. A* **605**, 191 (1996).
- [24] P. M. Jones, L. Wei, F. A. Beck, P. A. Butler, T. Byrski, G. Duchêne, G. de France, F. Hannachi, G. D. Jones, and B. Kharraja, *Nucl. Instrum. Methods Phys. Res., Sect. A* **362**, 556 (1995).
- [25] R. Fournier, J. Kroon, T. H. Hsu, B. Hird, and G. C. Ball, *Nucl. Phys. A* **202**, 1 (1973).
- [26] V. Paar, U. Eberth, and J. Eberth, *Phys. Rev. C* **13**, 2532 (1976).
- [27] M. Ivaşcu, N. Mărginean, D. Bucurescu, I. Căta-Danil, C. A. Ur, and Y. N. Lobach, *Phys. Rev. C* **60**, 024302 (1999).
- [28] V. Zobel, L. Cleemann, J. Eberth, T. Heck, and W. Neumann, *Nucl. Phys. A* **346**, 510 (1980).
- [29] F. Becker *et al.*, *Nucl. Phys. A* **626**, 799 (1997).
- [30] B. Singh and A. R. Farhan, *Nucl. Data Sheets* **107**, 1923 (2006).
- [31] J. F. Smith *et al.*, *Phys. Rev. Lett.* **75**, 1050 (1995).
- [32] S. Frauendorf and V. Pashkevich, *Phys. Lett. B* **141**, 23 (1984).
- [33] W. Nazarewicz and P. Olanders, *Nucl. Phys. A* **441**, 420 (1985).
- [34] M. S. Kaplan, J. X. Saladin, D. F. Winchell, H. Takai, and J. Dudek, *Phys. Rev. C* **44**, 668 (1991).
- [35] S. Skoda, F. Becker, T. Burkardt *et al.*, *Nucl. Phys. A* **633**, 565 (1998).
- [36] P. D. Cottle and O. N. Bignall, *Phys. Rev. C* **39**, 1158 (1989).
- [37] R. Han *et al.* (unpublished).
- [38] T. M. Shneidman, G. G. Adamian, N. V. Antonenko, R. V. Jolos, and W. Scheid, *Phys. Rev. C* **67**, 014313 (2003).
- [39] G. G. Adamian, N. V. Antonenko, R. V. Jolos, and T. M. Shneidman, *Phys. Rev. C* **70**, 064318 (2004).
- [40] T. M. Shneidman *et al.*, *Eur. Phys. J. A* **25**, 387 (2005).
- [41] T. M. Shneidman, G. G. Adamian, N. V. Antonenko, and R. V. Jolos, *Phys. Rev. C* **74**, 034316 (2006).
- [42] T. M. Shneidman, G. G. Adamian, N. V. Antonenko, R. V. Jolos, and S.-G. Zhou, *Phys. Rev. C* **92**, 034302 (2015).
- [43] T. Shneidman, G. Adamian, N. Antonenko, R. Jolos, and W. Scheid, *Phys. Lett. B* **526**, 322 (2002).
- [44] J. Maruhn and W. Greiner, *Z. Phys.* **251**, 431 (1972).
- [45] D. M. Brink, B. Buck, R. Huby, M. A. Nagarajan, and N. Rowley, *J. Phys. G* **13**, 629 (1987).
- [46] P. Möller, A. Sierk, T. Ichikawa, and H. Sagawa, *At. Data Nucl. Data Tables* **109**, 1 (2016).
- [47] A. Bohr and B. Mottelson, *Nuclear Structure* (Benjamin, New York, 1975), Vol. 2.
- [48] S. J. Q. Robinson, A. Escuderos, L. Zamick, P. von Neumann-Cosel, A. Richter, and R. W. Fearick, *Phys. Rev. C* **73**, 037306 (2006).
- [49] C. X. Yuan, C. Qi, and F. R. Xu, *Nucl. Phys. A* **883**, 25 (2012).
- [50] J. Adam, M. Honusek, A. Spalek, D. N. Doynikov, A. D. Efimov, M. F. Kudojarov, I. K. Lemberg, A. A. Pasternak, O. K. Vorov, and U. Y. Zhovliev, *Z. Phys. A* **332**, 143 (1989).
- [51] P. A. Butler, L. P. Gaffney, P. Spagnoletti *et al.*, *Phys. Rev. Lett.* **124**, 042503 (2020).
- [52] L. M. Robledo and P. A. Butler, *Phys. Rev. C* **88**, 051302(R) (2013).
- [53] K. Nomura, D. Vretenar, T. Nikšić, and B.-N. Lu, *Phys. Rev. C* **89**, 024312 (2014).
- [54] R. Rodríguez-Guzmán and L. M. Robledo, *Phys. Rev. C* **103**, 044301 (2021).
- [55] K. Nomura, R. Rodríguez-Guzmán, L. M. Robledo, and J. E. García-Ramos, *Phys. Rev. C* **103**, 044311 (2021).
- [56] K. Nomura, R. Rodríguez-Guzmán, L. M. Robledo, J. E. García-Ramos, and N. C. Hernández, *Phys. Rev. C* **104**, 044324 (2021).